Role of the Na^+-Ca^{2+} Exchanger as an Alternative Trigger of CICR in Mammalian Cardiac Myocytes

Chunlei Han, Pasi Tavi, and Matti Weckström
Department of Physical Sciences/Division of Biophysics, Department of Physiology, and Biocenter Oulu, University of Oulu, Finland

ABSTRACT Ca^{2+} influx through the L-type Ca^{2+} channels is the primary pathway for triggering the Ca^{2+} release from the sarcoplasmic reticulum (SR). However, several observations have shown that Ca^{2+} influx via the reverse mode of the Na^+-Ca^{2+} exchanger current ($I_{Na\text{-}Ca}$) could also trigger the Ca^{2+} release. The aim of the present study was to quantitate the role of this alternative pathway of Ca^{2+} influx using a mathematical model. In our model 20% of the fast sodium channels and the Na^+-Ca^{2+} exchanger molecules are located in the restricted subspace between the sarcolemma and the SR where triggering of the calcium-induced calcium release (CICR) takes place. After determining the strengths of the alternative triggers with simulated voltage-clamps in varied membrane voltages and resting $[Na]_i$ values, we studied the CICR in simulated action potentials, where fast sodium channel current contributes $[Na]_i$ of the subspace. In low initial $[Na]_i$ the Ca^{2+} influx via the L-type Ca^{2+} channels is the major trigger for Ca^{2+} release from the SR, and the Ca^{2+} influx via the reverse mode of the Na^+-Ca^{2+} exchanger cannot trigger the CICR. However, depending on the initial $[Na]_i$, the contribution of the Ca^{2+} entry via the exchanger may account for 25% (at $[Na]_i = 10$ mM) to nearly 100% ($[Na]_i = 30$ mM) of the trigger Ca^{2+}. The shift of the main trigger from L-type calcium channels to the exchanger reduced the delay between the action potential upstroke and the intracellular calcium transient. This may contribute to the function of the myocyte in physiological situations where $[Na]_i$ is elevated. These main results remain the same when using different estimates for the most crucial parameters in the modeling or different models for the exchanger.

INTRODUCTION

During an action potential in cardiac myocytes a small amount of Ca^{2+} enters the cells via L-type calcium channels. This triggers a larger amount of Ca^{2+} to be released from the sarcoplasmic reticulum (SR) (also called Ca^{2+}-induced Ca^{2+} release, or CICR; Fabiato and Fabiato, 1975). This causes a rise in $[Ca^{2+}]_i$, called the calcium transient, which is sufficient to produce contraction of the myocyte (Bers, 1993; Eisner et al., 1998). This view was first proposed by Fabiato (1985) based on a study with skinned cardiac muscles. Since then a close association has been documented between the amplitude of the L-type Ca^{2+} current and the amplitude of the Ca^{2+} transient (Beuckelmann and Weir, 1988; Näbauer et al., 1989). Studies of the elementary calcium release events, called Ca^{2+} sparks, indicate a tight functional connection between L-type Ca^{2+} channels and the calcium release channels, called ryanodine receptors (RyR). Due to the close proximity, the small amount of Ca^{2+} entering via the L-type Ca^{2+} channels is able to activate small clusters of RyR receptors and trigger the CICR (Lopez-Lopez et al., 1995; Cannell et al., 1995). Structural studies support this hypothesis by showing co-localization of the L-type Ca^{2+} channels and the RyR receptors in peripheral couplings of chicken cardiac muscle (Sun et al., 1995). Therefore, the interaction between the L-type Ca^{2+} channels and the RyR receptors takes place in a restricted subspace, or a microdomain (cleft space, or "fuzzy space"), where the concentrations of the key ions may change much more than in the bulk cytoplasm because of the limited possibilities for diffusion (Stern, 1992).

Although the important role of L-type Ca^{2+} current as a trigger of CICR in cardiac excitation-contraction (E-C) coupling is well-established, experimental data propose that Ca^{2+} entry via the reverse mode of the Na^+-Ca^{2+} exchanger could also contribute (Berlin et al., 1987; Bers et al., 1988; Leblanc and Hume, 1990; Lederer et al., 1990; Nuss and Houser, 1992; Levi et al., 1994; Lipp and Niggli, 1994). The ability of Na^+-Ca^{2+} exchange for triggering Ca^{2+} release from SR has been established in cardiac ventricular myocytes in a variety of species, such as rat (Wasserstrom and Vites, 1996), guinea pig (Sipido et al., 1997), and rabbit (Litwin et al., 1998). This is also supported by immunofluorescence labeling studies showing the existence of the Na^+-Ca^{2+} exchanger in the cardiac T-tubular system (Kieval et al., 1992; Frank et al., 1992). Controversially, some investigators have been unable to detect Ca^{2+} release from SR in the absence of L-type Ca^{2+} current (Näbauer et al., 1989; Sham et al., 1992; Evans and Cannell, 1997). Recent structural studies have shown in rat ventricular myocytes that, even when the Na^+-Ca^{2+} exchangers and Na^+ channels do not co-localize with the L-type Ca^{2+} channels and ryanodine receptors, they are present in the near vicinity, in the T-tubules (Scriven et al., 2000).

The quantitative description of the relationship between the Na^+-Ca^{2+} exchange and L-type Ca^{2+} channels in trig-

Submitted January 23, 2001, and accepted for publication December 3, 2001.

Address reprint requests to Dr. Matti Weckström, M.D., Dept. of Physical Sciences, Division of Biophysics, University of Oulu, P.O. Box 3000, 90014 Oulun yliopisto, Finland. Tel.: +358-8-537-5317; Fax: +358-8-537-5320; E-mail: matti.weckstrom@oulu.fi.

0006-3495/02/03/1483/14 $2.00

gering Ca^{2+} transient during cardiac action potential remains unclear. Experiments solving this question would require simultaneous measurement of at least Na^+-Ca^{2+} exchanger current ($\mu A/\mu F$) ($I_{Na\text{-}Ca}$), I_{Ca}, and $[Ca^{2+}]_i$, making it virtually insolvable. Another approach is to simulate experiments with a mathematical model. In the model of the subspace (dyadic cleft), Langer and Peskoff (1996) predict changes in sodium and calcium concentration in the vicinity of the center of the calcium release site that are large enough to cause a sizable exchanger current. The recently developed mathematical model of the cardiac myocyte (Jafri et al., 1998), also including the local control mechanism of the CICR, raises the possibility of quantitatively assessing, at the myocyte level, the role of the reverse mode of the Na^+-Ca^{2+} exchanger in triggering Ca^{2+} release from the SR. In the present study answers to the following were sought: 1) how much calcium the reverse mode of Na^+-Ca^{2+} exchange contributes to the triggering of the SR Ca^{2+} release; 2) under which conditions the Ca^{2+} entry through only the reverse exchange is able to trigger SR Ca^{2+}; and 3) how the CICR changes with increasing participation of the exchanger current.

METHODS

The modeling approach consists of numerically simulating a large group of differential equations that describe ion movements and storage, membrane currents and voltage, and especially calcium balance of the guinea pig ventricular myocyte. The model development was started from that of Luo and Rudy (1994) and Jafri et al. (1998), and extensive comparison to experimental data is to be found in those; we restrict treatment to the crucial parameters and results to those directly related to the problematics of the sodium-calcium exchanger as a trigger of CICR.

Based on the ultrastructural observations, Bers (1993) estimated that the ratios of the T-tubular system area/sarcolemmal area are 21% in rat ventricular myocytes, 37% in mouse ventricular myocytes, and 41% in rabbit ventricular myocytes. The ratios of the cleft area/T-tubular system area are quite close to this, 46% by Page (1978) and 48% by Langer and Peskoff (1996). Therefore, the cleft area/sarcolemmal area in the mammalian ventricle is likely to be in the range of 10–20%. We have used the high-end ratio (20%) in this simulation study. It is known that the T-tubular system has an abundance of Na^+-Ca^{2+} exchangers (Kieval et al., 1992; Frank et al., 1992). The two studies did not agree entirely with the distribution. Kieval et al. (1992) suggested that the exchanger is uniformly distributed in sarcolemmal membrane. Frank et al. (1992) suggested that the density of the exchanger is higher in the T-tubular area than in other parts. By assuming the uniform distribution of the fast sodium channels and the Na^+-Ca^{2+} exchanger in the sarcolemma, we introduced a fraction of 20% of the fast sodium channels and the Na^+-Ca^{2+} exchangers to the restricted subspace in the model.

With the modification described above we had to find the suitable time constant for sodium diffusion from the restricted subspace to bulk cytoplasm. In the model of Jafri et al. (1998) the time constant for calcium diffusion from the subspace to bulk cytoplasm is 3.125 ms. Generally, sodium diffusion should be much faster than calcium in water due to its smaller diameter. However, in cytoplasm the diffusion is likely to be substantially slower. Wendt-Gallitelli et al. (1993) estimated that the sodium diffusion coefficient in the restricted subspace is approximately equal to 1% of its value in water, and Kabakov (1998) estimated this value as $<0.001\%$ of its value in water. Much slower diffusion time constants of up to several tens of seconds may be inferred from the experimental data by Fujioka et al. (1998). In our model we introduced 2 ms as the time constant for sodium diffusion from restricted subspace to bulk cytoplasm, and this may be taken as a lower, conservative limit for the diffusion speed. Slower diffusion (larger time constants) would exaggerate the effect of the exchanger as trigger of Ca^{2+} release.

Fig. 1 *A* shows a scheme of the myocyte model, and Fig. 1 *B* shows the Ca^{2+} and Na^+ fluxes contributing to their concentrations in cleft space: 1) I_{ss}, the Ca^{2+} influx of two components, the L-type Ca^{2+} channel and the Na^+-Ca^{2+} exchanger; 2) J_{xfer}, the Ca^{2+} diffusing from the subspace to bulk cytoplasm; and 3) J_{rel}, the Ca^{2+} flux from SR to the subspace. With the model it is possible to define thresholds for triggering the CICR in the subspace: 1) the threshold of local Ca^{2+} concentration in subspace ($[Ca]_{ss,th}$); and 2) the threshold of Ca^{2+} influx through sarcolemma for triggering the CICR process ($I_{ss,th}$), which includes two components, the Ca^{2+} currents via the L-type Ca^{2+} channel and via the reverse mode of the Na^+-Ca^{2+} exchanger. We defined these two thresholds by clamping them (i.e., keeping them at a forced value, keeping all other variables constant). After the duration-density curves were plotted, they were fitted to the equation

$$d = \frac{B}{(y - y_o)^n} \tag{1}$$

where y is $I_{ss,th}$ or $[Ca]_{ss,th}$, y_0 is the minimum threshold of $I_{ss,th}$ or $[Ca]_{ss,th}$, d is the duration for clamping time, and n and B are characteristic parameters for describing this curve. This equation is usually used for studying the action potential thresholds of excitable cells with $n = 1$. In this study, however, the exponent was allowed to vary because there is no a priori reason to assume the value of unity of the exponent.

The original Luo-Rudy formulation of the Na^+-Ca^{2+} exchanger did not include binding reactions of the ions to the exchanger, but relies on the Goldman-Hodgkin-Katz (GHK) current equation that is not able to reproduce, e.g., saturation. To study possibly different predictions of the Luo-Rudy formulation (non-kinetic model) as compared to a kinetic model of the exchanger, we used an alternative formulation of the exchanger function (Matsuoka and Hilgemann, 1992). The Hilgemann model is a state-dependent model including modeling of the binding kinetics of the ions to the exchanger. The formulation involves differential equations for the shifts of the molecule between states. We used the four-state model of Matsuoka and Hilgemann (1992) (Fig. 1 *C*), and the exchanger current then becomes

$$I_{Na,Ca} = K(E_n \cdot k_{n,n-1} - E_{n-1} \cdot k_{n-1,n}) \tag{2}$$

where K is a scaling factor (60.8 $\mu A/\mu F$) necessary to scale the ionic flux with unknown amounts of the exchanger in different states into experimentally found membrane current, E_n and E_{n-1} are the fractional amounts of the exchanger in any two successive states, and the $k_{n,n-1}$ and $k_{n-1,n}$ are the corresponding rate constants.

All the simulations in the present study were performed with a program developed in MATLAB v.5.0 ODE (ordinary differential equation) suite (The Math Works Inc., Natick, MA) using a PC (Pentium II 233) and a Sun Workstation.

RESULTS

The trigger thresholds of CICR in simulation study

In all of the following simulations the formulation of the Na^+-Ca^{2+} exchanger has been the numerical approximation used in the Luo-Rudy model, based on the GHK current

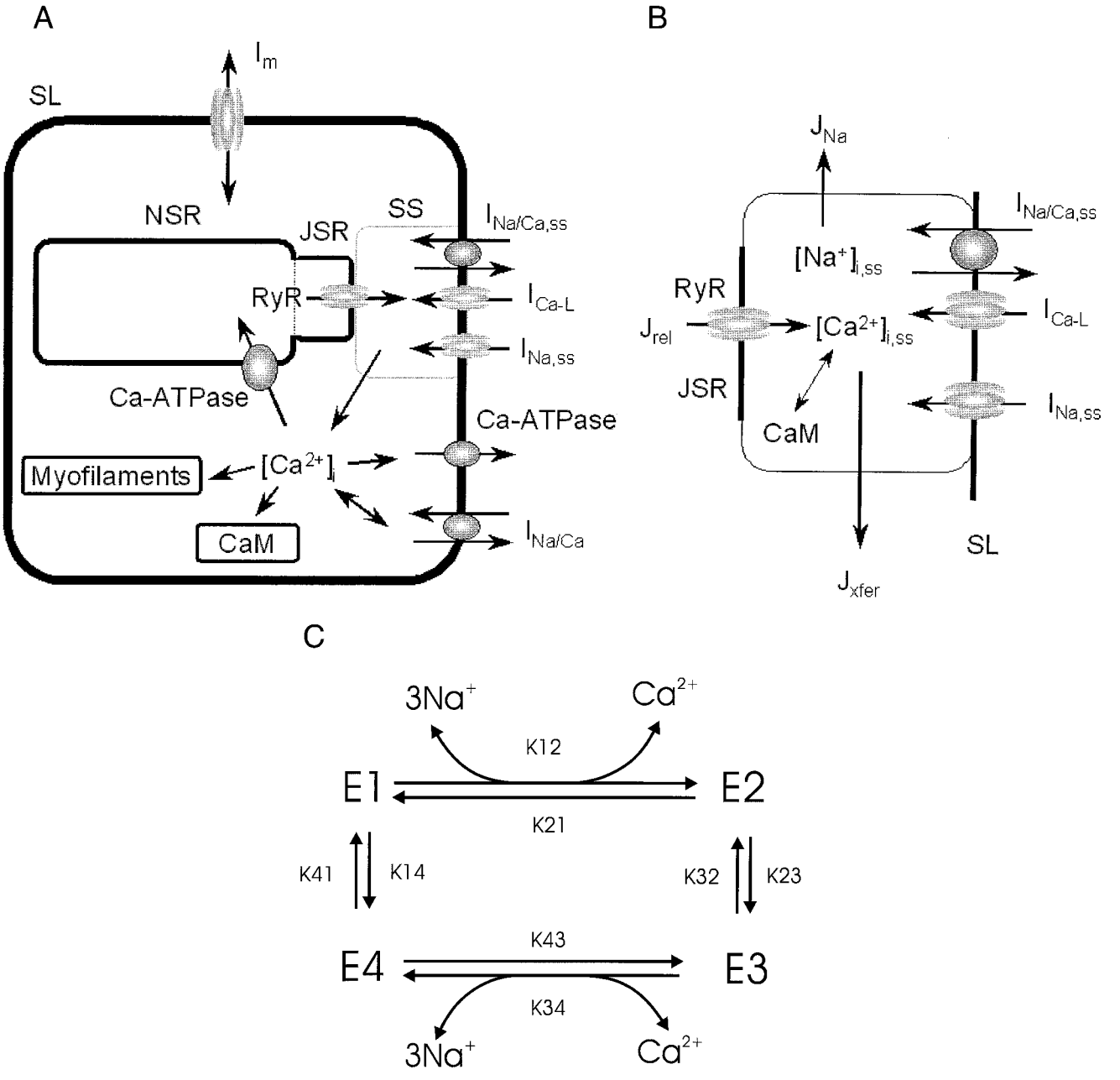

FIGURE 1 Description of the mathematical model used, and of its components. (*A*) Schematic diagram of the cell model that was built from the basis of that published by Jafri and co-workers (1998). The main differences from the cited model are that 20% of the Na^+-Ca^{2+} exchangers ($I_{Na/Ca}$) and fast sodium channels are located in the sarcolemma of the restricted subspace. I_m, the sarcolemmal ionic currents, including all currents through the voltage-gated channels (for details, see Methods); NSR, network SR; JSR, junctional SR; SL, sarcolemma; SS, the restricted subspace compartment where the coupling between the L-type calcium current (I_{Ca-L}) and the calcium release from the SR through the ryanodine receptors (RyR) takes place; $I_{Na,ss}$, the Na^+ current into the subspace via fast sodium channels; $I_{Na/Ca,ss}$, the Na^+/Ca^{2+} exchanger current in the subspace membrane; Ca-ATPase, the ATP-driven transport of Ca^{2+} out of the cytoplasm; CaM, calmodulin that is one of the main Ca^{2+} buffers in cytoplasm. (*B*) The ion flux components in the restricted subspace. Fast Na^+ channels ($I_{Na,ss}$), L-type Ca^{2+} channels, and Na^+-Ca^{2+} exchangers are located in the sarcolemma and the ryanodine receptors in the sarcoplasmic reticular membrane. Sodium and calcium ions diffuse from the subspace to the cytoplasm. There are three calcium ion flux components into or from the subspace, defined as: 1) I_{ss}, the total transsarcolemmal Ca^{2+} influx into restricted subspace, consisting of two parts, the I_{Ca-L} (L-type Ca^{2+} current) and $I_{Ca/Na,ss}$ (Ca^{2+} flux via Na^+-Ca^{2+} exchanger); 2) J_{rel}, Ca^{2+} release via RyR receptor from SR; 3) J_{xfer}, Ca^{2+} diffusion from the subspace to the bulk cytoplasm. Note that in this modified model no specific coupling between RyR receptors and L-type Ca^{2+} channels or Na^+-Ca^{2+} exchangers was assumed. This means that the RyR receptors respond to the elevation of Ca^{2+} concentration in the restricted subspace. Other symbols as in *A*. (*C*) A simplified diagram of the implementation of the kinetic, state-dependent model of the Na^+/Ca^{2+} exchanger function as suggested by Matsuoka and Hilgemann (1992; their model with four states). E_1–E_4: different states of the exchanger molecule; k_n, n-1, and $k_{n\text{-}1,n}$: the forward and reverse rate constants of the shifts of the exchanger between states, where n, s correspond to the states of the molecule. The states E_1 and E_2 react with sodium and calcium on the outside of the membrane, and states E_3 and E_4 on the inside.

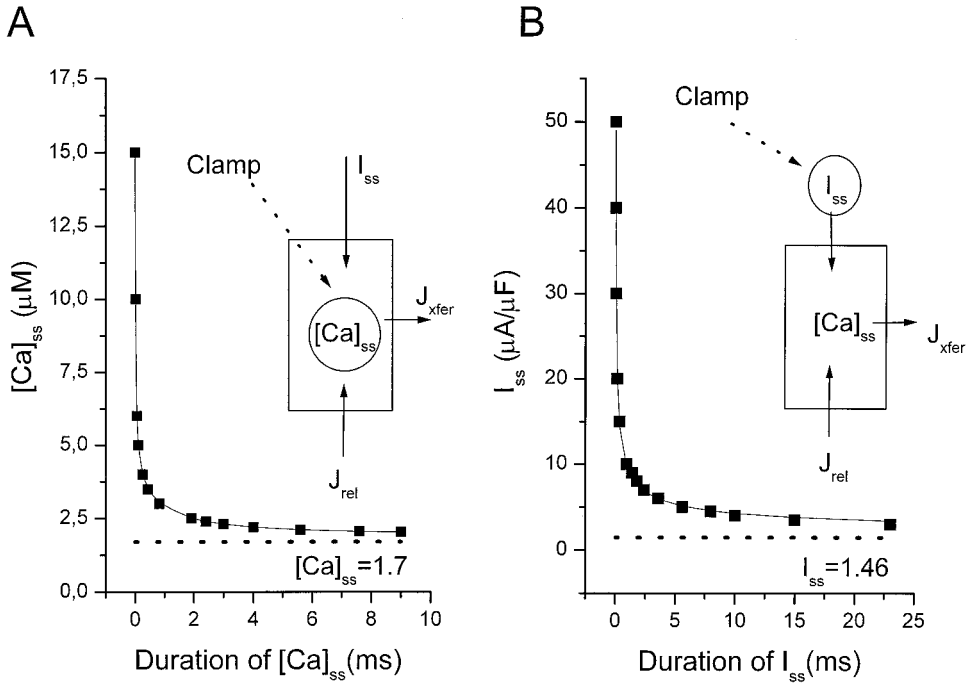

FIGURE 2 The duration-density relationships of $[Ca]_{ss}$ and I_{ss} for triggering the Ca^{2+} release from SR in the subspace. The data are fitted to $d = B/(y - y_0)^n$ (see details in Materials and Methods). Insets show the simulation protocols. Above the curves the CICR is triggered, and below it is not. (*A*) Calcium concentration in the subspace $[Ca]_{ss}$ is "clamped." When the duration and value of the calcium concentration are varied and the presence or absence of calcium transients observed, we obtain the minimum value of $[Ca]_{ss}$ that is able to trigger CICR. The dashed line indicates that Ca^{2+} release could be triggered only after Ca^{2+} concentration in restricted subspace reaches values of over 1.7 μM (equal to the estimated value of $[Ca]_{ss}$ that would be effective after an unlimited time, $n = 3.3$, $B = 5.4$). Above this threshold, the time needed for triggering Ca^{2+} release from SR decreased with increase of $[Ca]_{ss}$. (*B*) The calcium influx into the subspace (I_{ss}) is clamped and varied in the similar manner as the calcium concentration in *A*. The dashed line indicates that Ca^{2+} release could be triggered only after Ca^{2+} influx via sarcolemma to restricted subspace was >1.46 μA/μF, and above this threshold, the time needed for triggering Ca^{2+} release from SR decreased with the increasing the I_{ss}.

equation. Two thresholds may be defined for triggering of the CICR (as explained in Methods), namely $I_{ss,th}$, the threshold of Ca^{2+} influx through the sarcolemma, and $[Ca]_{ss,th}$, the threshold of local Ca^{2+} concentration in subspace. By forcing (i.e., "clamping") the subspace Ca^{2+} concentration $[Ca]_{ss}$ and the Ca^{2+} influx current I_{ss} to selected values in the model and varying the corresponding duration (horizontal axis in Fig. 2, *A* and *B*), we produced functions reminiscent of the strength-duration of chronaxie-curves (e.g., Ganong, 1977) originally defined for the excitability of the membranes. The clamping of the $[Ca]_{ss}$ (the vertical axis in Fig. 2 *A*) shows that the CICR could be triggered when the Ca^{2+} concentration in subspace is >1.7 μM (Fig. 2 *A*). For $[Ca]_{ss}$ to reach the level of $[Ca]_{ss,th}$ in the subspace, the transsarcolemmal inward Ca^{2+} current (I_{ss}, vertical axis in Fig. 2 *B*) needed to be at least 1.46 μA/μF.

The sodium dependence of the *I-V* relationships of $I_{Ca,L}$ and Na^+-Ca^{2+} exchange

Fig. 3 *A* shows the *I-V* relationship of Ca^{2+} current through L-type Ca^{2+} channels (μA/μF; $I_{Ca,L}$) obtained by voltage-clamp simulation. This reproduces the experimentally defined bell-shaped relation between $I_{Ca,L}$ and voltage, with peak amplitude at ~0 mV. The Ca^{2+}-dependent inactivation is also modeled here (following Jafri et al., 1998) by simulating the switch from the normal to the inactivated mode by Ca^{2+} binding to the channel receptors. The effects of Ca^{2+}-dependent inactivation to peak current of $I_{Ca,L}$ are shown clearly in Fig. 3 *A*. The Ca^{2+} current through the Na^+-Ca^{2+} exchanger ($I_{Ca,Na-Ca}$; $I_{Ca,Na-Ca} = 2\ I_{Na-Ca}$ (μA/μF)) was simulated in different intracellular calcium and sodium concentrations (Fig. 3 *B*). Because the Na^+-Ca^{2+} exchanger transports 3 Na^+ for 1 Ca^{2+}, the amplitude of the calcium current through the exchanger should be two times as large as the exchanger current (I_{Na-Ca}) itself and in opposite direction, i.e., the calcium part of the current.

In the membrane voltage range reached by action potentials in cardiac myocytes, $I_{Ca,Na-Ca}$ is affected by both $[Ca]_i$ and $[Na]_i$. Intracellular calcium mainly affects the normal mode of the Na^+-Ca^{2+} exchanger and, accordingly, the $I_{Ca,Na-Ca}$ depends on the $[Ca]_i$ at negative membrane potentials. Intracellular sodium mainly affects the reverse mode of $I_{Ca,Na-Ca}$, and shifts the reversal potential to more negative membrane voltages. When the $[Na]_i$ is increased (Fig. 3

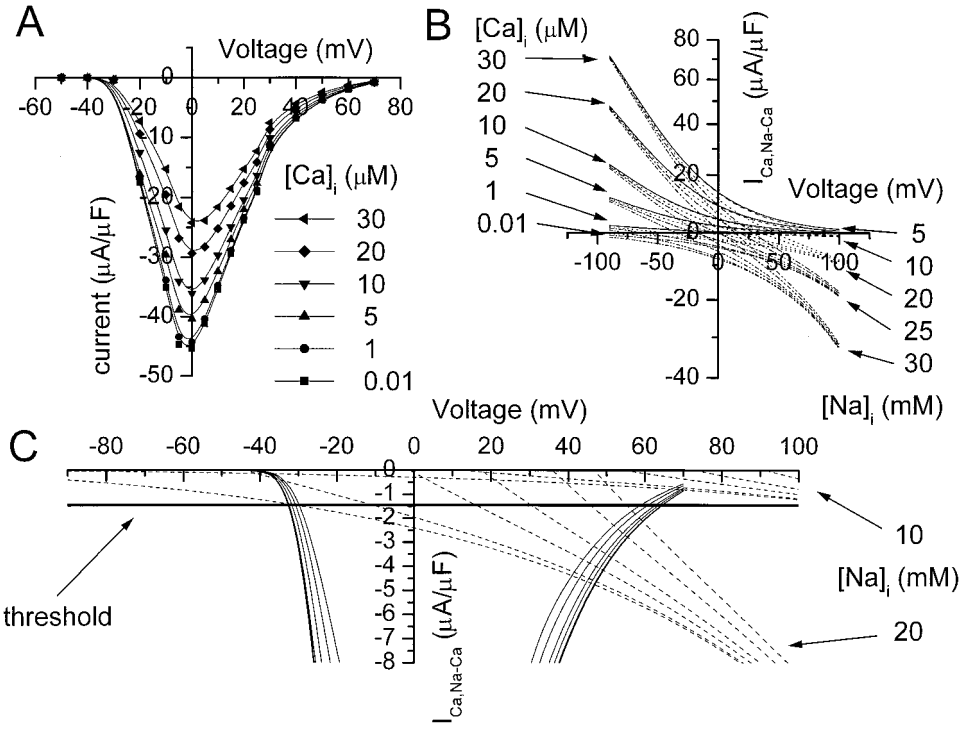

FIGURE 3 The current-voltage (*I-V*) characteristics of the L-type Ca^{2+} current and the reverse mode of the Na^+-Ca^{2+} exchanger in varying intracellular concentrations of calcium and sodium. (*A*) The *I-V* relation of the L-type Ca^{2+} current in different intracellular Ca^{2+} concentration (from 0.01 to 30 μM, as indicated by different symbols). (*B*) The *I-V* relation of the Ca^{2+} flux via Na^+-Ca^{2+} exchanger ($I_{Ca,Na\text{-}Ca}$) and its dependence on $[Ca]_i$ and $[Na]_i$. Because the ratio of the exchange for the Na^+-Ca^{2+} exchanger is 3 Na^+:1 Ca^{2+}, the current becomes $I_{Ca,Na\text{-}Ca} = -2I_{Na\text{-}Ca}$. First, the $[Na]_i$ has a large influence on the $I_{Ca,Na\text{-}Ca}$ at very positive membrane potentials (from $\sim$+50 to 100 mV), where $[Ca]_i$ has little effect, and thus the curves tend to converge. Second, $[Ca]_i$ mainly influences $I_{Ca,Na\text{-}Ca}$ at fairly negative potentials (from -50 to -90 mV), where $[Na]_i$ has little influence, and the curves again tend to converge. $[Ca^{2+}]$ and $[Na^+]$ concentrations used are shown beside the corresponding curves. (*C*) Combination of the two *I-V* relation curves ($I_{Ca,L}$ and $I_{Ca,Na\text{-}Ca}$) and a comparison with the $I_{ss,th}$ (the threshold of Ca^{2+} influx via the sarcolemma to the restricted subspace for triggering the Ca^{2+} release via RyR receptor from SR; continuous horizontal line). All values of the *I-V* curves below the threshold will cause CICR. Note that $I_{Ca,Na\text{-}Ca}$ is always smaller than the threshold ($I_{ss,th}$) when $[Na]_i$ is 10 mM, but $I_{Ca,Na\text{-}Ca}$ is significantly larger with increasing $[Na]_i$ from 10 to 20 mM.

B) the current density of $I_{Na\text{-}Ca}$ increases, and its reversal potential shifts to more negative values, suggesting that $[Na]_i$ plays an important role in determining the conditions under which the exchanger current could trigger the Ca^{2+} release from SR in cardiac myocytes. This is evident when the L-type Ca^{2+} channel current and $I_{Ca,Na\text{-}Ca}$ are plotted together (Fig. 3 *C*), combined with a line showing the threshold current of calcium needed to trigger the Ca^{2+} release from the SR (see Fig. 2 *B*). With low sodium (10 mM), and with the membrane potential at -30 mV, $I_{Ca,L}$ reached the threshold ($I_{ss,th}$), but $I_{Ca,Na\text{-}Ca}$ was below the threshold even when the potential was at +100 mV. $I_{Ca,Na\text{-}Ca}$ was not large enough to trigger CICR in low $[Na]_i$, but its contribution increased in the function of the increasing $[Na]_i$. With $[Na^+]_i$ at 20 mM, the calcium current via the exchanger reached the threshold at all voltages between -30 mV and +55 mV, depending on $[Ca^{2+}]_i$ (Fig. 3 *C*). With $[Ca]_i$ at 1 μM, $I_{Ca,Na\text{-}Ca}$ reached the threshold at -12 mV, but it was still smaller than the L-type current.

Voltage-clamp simulations

On the basis of the *I-V* curves of the L-type calcium channel and Na^+-Ca^{2+} exchanger (Fig. 3), one would draw the conclusion that the possibility of the Na^+-Ca^{2+} exchanger current inducing CICR in the presence of functional L-type channels is very small. However, the *I-V*-relationships yields information about neither the synergism of the two triggers nor of the triggered event itself, the Ca^{2+} transient. The question is also complicated by the cumulative nature of the trigger, i.e., Ca^{2+} accumulation in the subspace (Fig. 2). Therefore, we further studied the question by simulation of voltage-clamp experiments with the model cell.

In the voltage-clamp simulations (Figs. 4 and Fig. 5), the holding potential was set to -40 mV to inactivate the fast sodium channels and avoid (at this stage) the more complex contribution of changes in intracellular $[Na^+]_i$. The command potential (Fig. 4, *A* and *E*) was varied from -30 to +50, with 10-mV steps of 150-ms duration. The

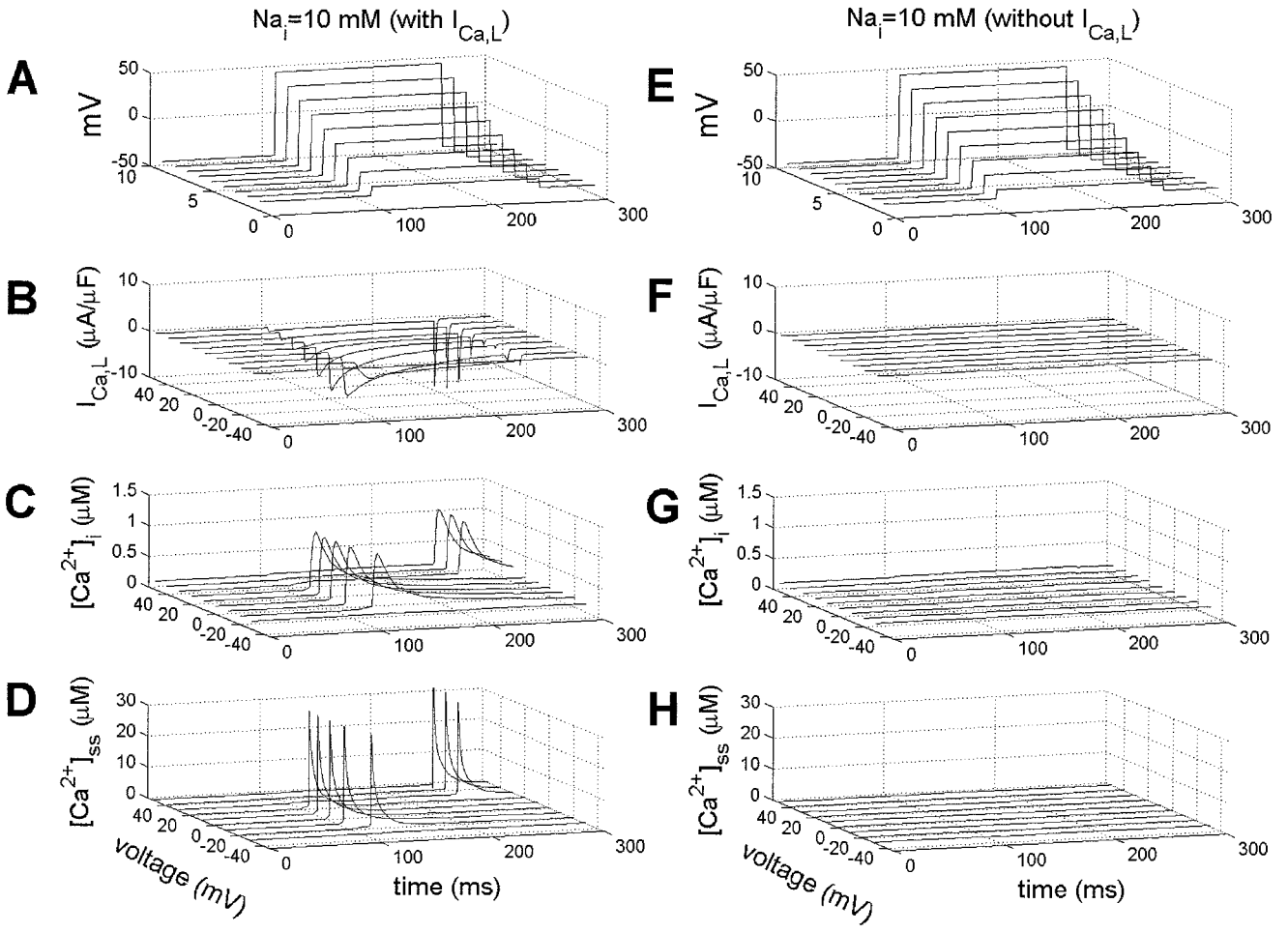

FIGURE 4 Examination of the calcium release in a voltage-clamp simulation in the presence (*A–D*) and absence (*E–H*) of L-type Ca^{2+} channels while $[Na]_i = 10$ mM. (*A*) The voltage-clamping protocol; (*B*) calcium current via the Na^+/Ca^{2+} exchanger, $I_{Ca,Na\text{-}Ca,ss}$; (*C*) calcium concentration in cytoplasm $[Ca]_i$; (*D*) calcium concentration in the subspace $[Ca]_{ss}$. (*E–H*) Corresponding figures in the absence of L-type Ca^{2+} current. Holding potential is −40 mV, command potential from −30 to +50 mV, step = 10 mV. The Ca^{2+} transients can be triggered at most command potentials (from −10 to +20 mV) when the L-type Ca^{2+} channels are functional. Without the L-type Ca^{2+} channels no Ca^{2+} transients are triggered.

voltage commands activated the L-type current (Fig. 4 *B*). With intracellular sodium concentration of 10 mM (as in Fig. 4), the calcium release from SR can be triggered in most command voltages (from −20 to +20 mV), as seen in the cytosolic calcium transients in Fig. 4 *C* and the subspace transients in Fig. 4 *D*. When the L-type channel activation was omitted from the model (no current in Fig. 4 *F*), no calcium release was observed at any of the command voltages under these conditions (Fig. 4, *G* and *H*). Note that the large tail-current of the $I_{ca,L}$ induced with the three largest amplitudes of the command voltage (Fig. 4 *B*) caused a full-grown calcium transient.

With significantly higher $[Na^+]_i$ at 17 mM the calcium release was triggered without L-type calcium channels with the same set of command voltages as in Fig. 4. This is seen as calcium transients in the subspace (Fig. 5 *B*) and in the cytoplasm (*C*). As shown by Fig. 5, *B* and *E*, depicting the Ca^{2+} concentration in the subspace, the trigger in this situation is the calcium accumulating into the subspace via the reverse-mode current of the Na^+-Ca^{2+} exchanger ($I_{Ca,Na\text{-}Ca,ss}$, Fig. 5, *A* and *D*). Examination of this Na^+-Ca^{2+} exchanger-induced calcium release (evident in Fig. 5, *D* and *E* showing $I_{Ca,Na\text{-}Ca}$, and Ca_{ss} in expanded vertical scale) reveals that Ca^{2+} transients were found to be triggered significantly faster in the function of the increasing depolarization. The delay between the depolarization and the onset of the calcium transient showed clear sodium dependence, as seen in Fig. 5 *F*, which shows the delay in the onset of calcium release in the function of command voltage at different intracellular sodium concentration. At 22 mM of $[Na^+]_i$ the delay was ~5 ms (at +50 mV command voltage), whereas the corresponding value at 10 mM of $[Na^+]_i$ was 29 ms. The sodium-dependent shift in delay induced by the Na^+-

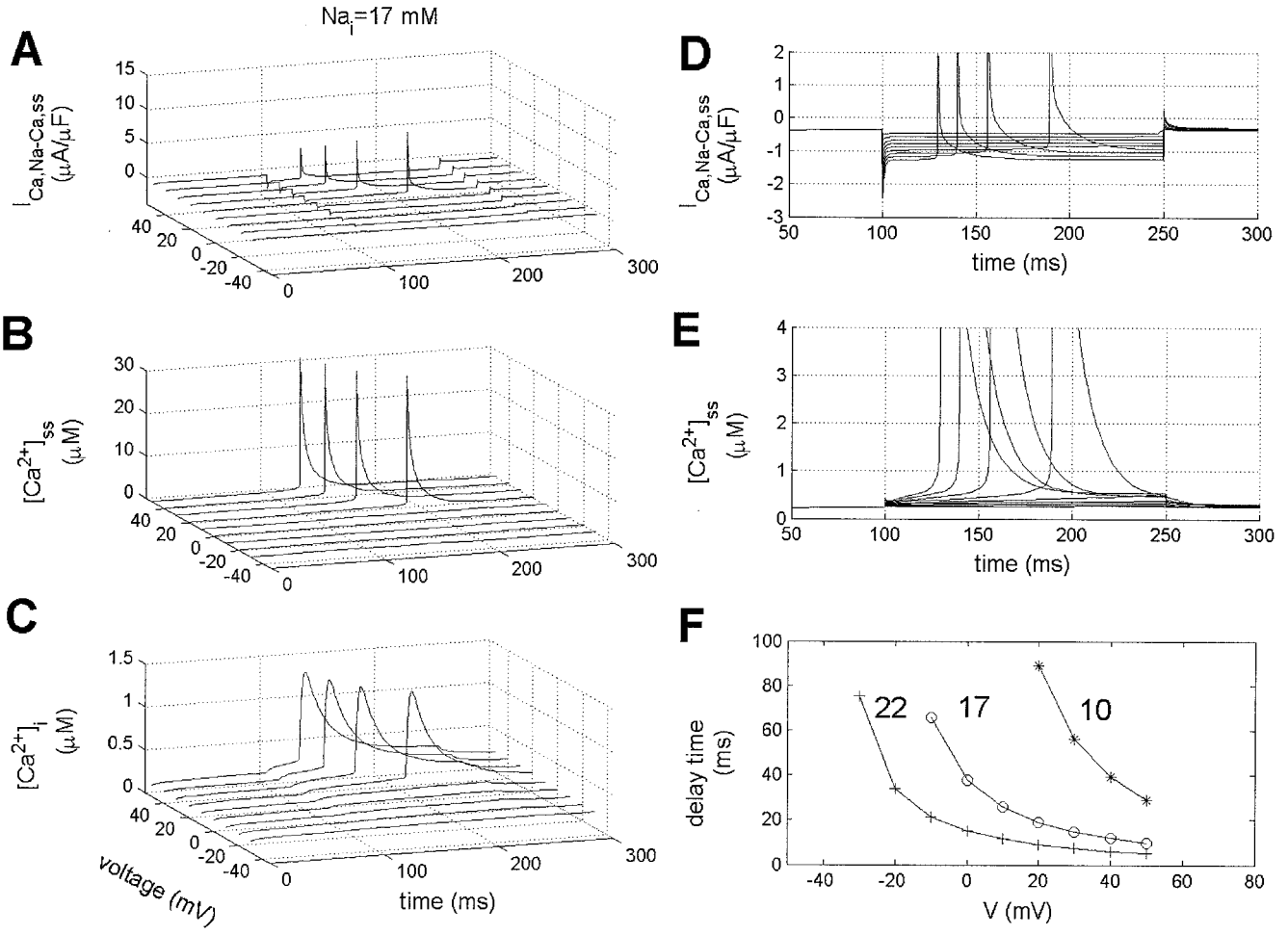

FIGURE 5 Voltage-clamp simulation with increased $[Na]_i$ (17 mM) and without functional L-type calcium current. The voltage-clamp protocol is the same as in Fig. 4. (*A*) $I_{Ca,Na-Ca}$; (*B*) calcium concentration in subspace $[Ca]_{ss}$; (*C*) calcium concentration in the cytoplasm $[Ca]_i$. With increased intracellular sodium the Ca^{2+} releases are now triggered. (*D* and *E*) A closer examination of the $I_{Ca,Na-Ca}$ and the $Ca_{ss.}$ Note that the calcium transients (*E*) are triggered at different times after the beginning of the stimulus pulse (at 100 ms), depending on the amplitude of the voltage pulse. (*F*) The sodium- and voltage-dependence of the delay for triggering Ca^{2+} release from intracellular calcium stores with the presence of L-type Ca^{2+} channels. The delay time is defined as the duration between depolarization (leading edge of the voltage-clamp pulse) and the onset of the calcium transient. The delay is shown for three different levels of $[Na]_i$: (∗) 10 mM, (○) 17 mM, and (+) 23 mM.

Ca^{2+} exchanger current opens the possibility that the Na^+-Ca^{2+} exchanger current precedes the L-type calcium current at high $[Na^+]_i$. This means that the (main) trigger of CICR could be changed upon accumulation of sodium.

Role of the Na^+/Ca^{2+} exchanger as a CICR trigger during action potential

On the basis of the voltage-clamp simulations, the reverse mode of the Na^+/Ca^{2+} exchanger contributes to CICR in a sodium-dependent manner. However, during normal APs the $[Na^+]_i$ is also influenced by the fast sodium current. To investigate this, we performed model simulations at varying $[Na]_i$ (10, 13, 17, 20, and 22 mM). Fig. 6 *A* shows a simulated action potential with corresponding changes in the Na^+-Ca^{2+} exchanger current (Fig. 6 *B*), sodium concentration $[Na]_{ss}$ in the subspace (Fig. 6 *C*), the calcium transients in subspace ($[Ca]_{ss}$) (Fig. 6 *D*), the calcium component of the Na^+/Ca^{2+} exchanger current in subspace membrane, $I_{Na,Na-Ca,ss}$ (Fig. 6 *E*), and the L-type calcium channel current in subspace membrane (Fig. 6 *F*). Insets show the early events during the first 5 ms in an expanded time scale. As expected, the AP duration and amplitude decreased upon increase of the initial $[Na]_i$. This effect is due to the increased Na^+/Ca^{2+}-exchanger outward current (Fig. 6 *B*), reflecting the increased calcium influx during early phases of the upstroke of the AP (Fig. 6, *E* and *F*). In these simulations we observed the same phenomenon as

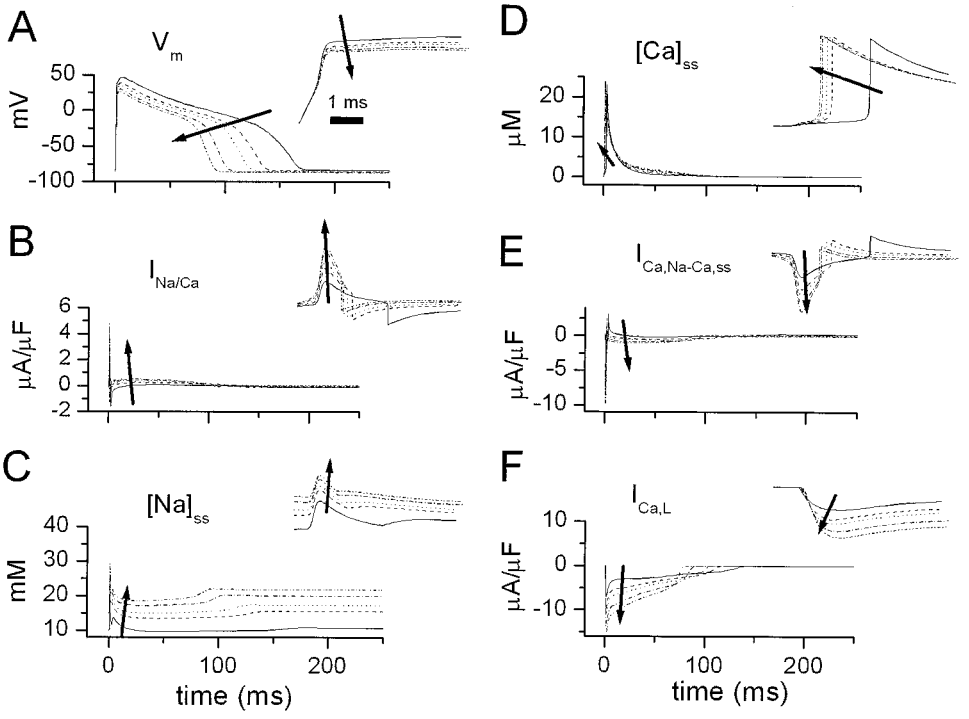

FIGURE 6 Calcium concentrations and currents during action potentials (L-type current functional) at varied concentrations of $[Na]_i$ (*arrows* show the direction of the change in function of the increased intracellular sodium. In all figures this is in the order 10, 13, 17, 20, 22 mM with corresponding styles of *solid*, *dashed*, *dotted*, *dash-dotted*, and *dash-double-dotted* lines). (*A*) Action potential; (*B*) $I_{Na\text{-}Ca}$; (*C*) subspace concentration of sodium $[Na]_{ss}$; (*D*) $[Ca]_{ss}$; (*E*) $I_{Ca,Na\text{-}Ca}$; (*F*) $I_{Ca,L}$. Insets show the early events during the first 5 ms in an expanded time scale (horizontal scale bar = 1 ms; vertical scale remains the same).

seen in the voltage-clamp experiments, namely that at high $[Na^+]_i$ the dominant trigger of the CICR is shifted from the L-type current toward the Na^+/Ca^{2+} exchanger current. This is also contributed by the sodium current, which is able to increase the $[Na^+]_{ss}$ transiently to ~20 mM in normal $[Na^+]_i$ (Fig. 6 *C*). In high $[Na^+]_i$ the peak $[Na^+]_{ss}$ reaches 30 mM, augmenting the exchanger current (Fig. 6, *B* and E). As a result, the delay between the depolarization and subspace Ca^{2+}-transient is greatly reduced (Fig. 6 *D*, *inset*). The small voltage-dependent inactivation of the L-type channels explains the paradoxical increase of the L-type current during lower voltage (i.e., reduced AP peak voltage) in Fig. 6 *F*.

As determined earlier (Fig. 2), the triggering event of CICR can be characterized by calcium accumulation into the subspace, i.e., calcium flux per time. The estimation of the trigger efficiency of L-type calcium current and Na^+/Ca^{2+} exchanger current would be best evaluated by comparing the time integral of the currents. To do so, the Ca^{2+} entering the cell through either the L-type channels or via the exchanger current was calculated by integrating the Ca^{2+} currents from the start of the action potential to the activation of SR ryanodine receptors (Fig. 7). The contribution of the exchanger to the SR Ca^{2+} release (Fig. 7 *D*) is the ratio of the integration of Ca^{2+} component of the exchange with the sum of Ca^{2+} entry via two pathways, i.e., via L-type Ca^{2+} and the reverse mode of the Na^+-Ca^{2+} exchange. Upon increase of the $[Na^+]_i$ (as indicated by the arrows), the subspace calcium transient is triggered faster than previously (Fig. 7 *A*), as found in the previous sections (see Figs. 5 and 6). As seen from the Fig. 7 *C*, subspace exchanger current dominates this phenomenon, being activated more rapidly than subspace L-type current (Fig. 7 *B*) upon sodium increase. Therefore, the contribution of the exchange to SR Ca^{2+} release is 25% in normal $[Na]_i$, and the contribution of the exchange increases to 40%, 52%, 67%, and 73% when $[Na]_i$ increased to 13, 17, 20, and 22 mM, respectively (Fig. 7 *D*). In extreme situations ($[Na]_i$ = 30 mM) the contribution of the Na^+-Ca^{2+} exchange is almost 100%.

Use of a state-dependent model of the exchanger

In the simulations above the function of the Na^+-Ca^{2+} exchanger was modeled according to the Luo-Rudy model. Because in this formulation no binding of Na^+ and Ca^{2+} is involved, the model does not predict any saturation of the exchanger current at high $[Na^+]_i$ and

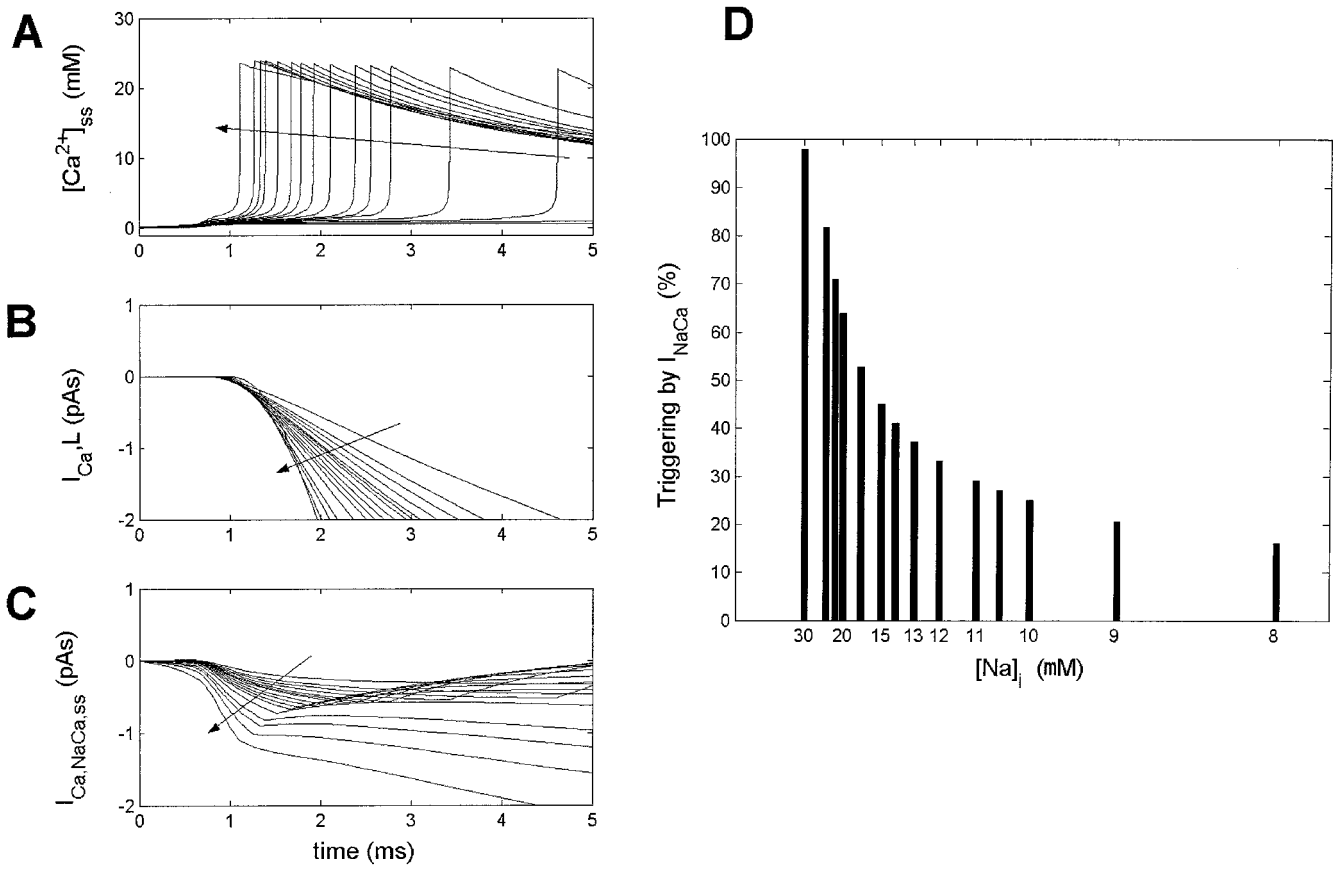

FIGURE 7 The cumulative effect of the two sources of calcium influx at varied $[Na]_i$ (concentrations shown in *D*). The arrows show the change in function of increasing $[Na]_i$. (*A*) Action potentials with $[Na]_i$ increased from 8 to 30 mM. (*B*) Integral of Ca^{2+} entry through L-type Ca^{2+} channels ($\int I_{Ca}(t)dt$); (*C*) Integral of Ca^{2+} entry through the exchanger ($\int I_{Ca,Na\text{-}Ca}(t)dt$). (*D*) Contribution of the Na^+-Ca^{2+} exchanger-mediated calcium inward current for triggering the SR Ca^{2+} release. The contribution (as percent) of the exchanger is defined as the ratio of the integrated Ca^{2+} component of the exchanger to the sum of the Ca^{2+} entry via two pathways (via the L-type Ca^{2+} channels and Na^+-Ca^{2+} exchanger).

$[Ca^{2+}]_i$, and errors or instability in simulations are possible, as suggested by Varghese and Sell (1997). With an alternative formulation, a state-dependent model of the exchanger function (Matsuoka and Hilgemann, 1992), it was possible to include binding kinetics of the ions to the exchanger.

To test the difference between the two exchanger models in triggering calcium release from SR, we first compared the steady-state current-voltage relations of the exchanger in two models. Furthermore, we explored the relative role of calcium entry through the exchanger as a trigger for calcium release (similar to the above, in Fig. 7 *D*). In the Hilgemann model the steady-state solution (Matsuoka and Hilgemann, 1992) and a scaling factor of 60.8 μA/μF is used, giving a membrane current (Fig. 8 *A*) roughly consistent with experimental data. At high positive membrane voltage and $[Na^+]_i$, the $I_{Na/Ca}$ generated by the Hilgemann model showed saturation (Fig. 8 *A*) not present in the Luo-Rudy model (Fig. 8 *B*). In the physiologic range of $[Na^+]_i$ (~10 mM) the high positive membrane voltage elicits a larger outward current in the Hilgemann model than in the Luo-Rudy model. At $[Na^+]_i$ = 10 mM, $[Ca^{2+}]_i$ = 0.1 μM, and V_m = 40 mV, we obtained $I_{Na/Ca}$ of 4.3 μA/μF with the Hilgemann model, but only 1.0 μA/μF with the Luo-Rudy model. Based on these data it is clear that the calcium entry via the reversal mode of the exchanger contributes much more for the triggering of calcium release (Fig. 8 *C*) in the Hilgemann model when compared with the Luo-Rudy model (55.6% vs. 20.5%) under otherwise identical conditions. Observing that the Hilgemann model overestimates the exchanger current in moderately positive membrane voltages (compare Fig. 8, *A* and *B*), we may reduce the simulated exchanger current by decreasing the scaling factor (see Methods). This is shown in Fig. 8 *C* above the columns (the value 1 being equal to the original formulation). Thus, the Hilgemann model yields the same relative contribution as the Luo-Rudy model only if this factor is 0.2; therefore we can conclude that using an alternative model for the exchanger current leads to even

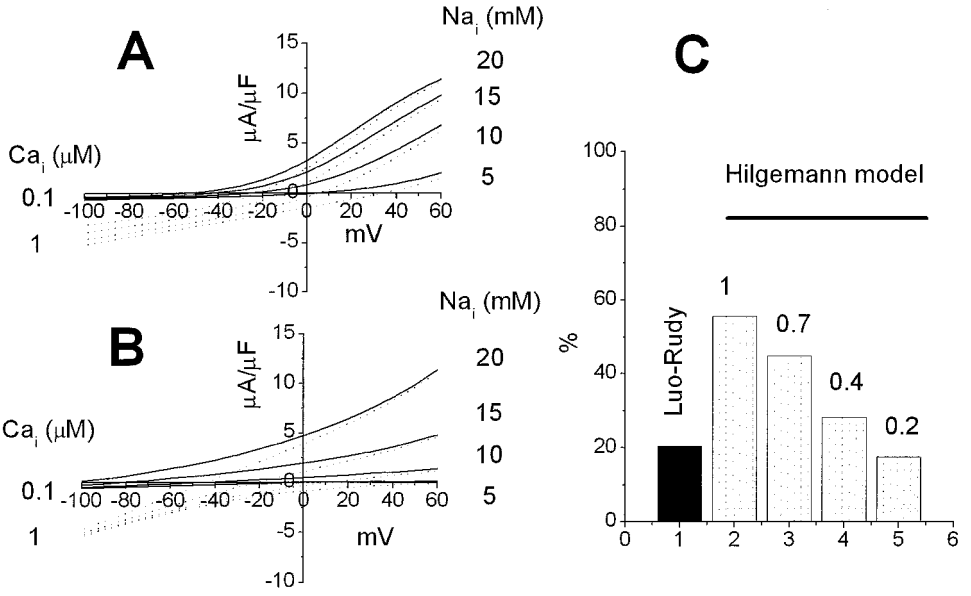

FIGURE 8 Comparison of the Hilgemann model (Matsuoka and Hilgemann, 1992) with the Luo-Rudy formulation of the Na^+-Ca^{2+} exchanger current. The current-voltage relationship curves given by the models. (*A*) Hilgemann model; (*B*) Luo-Rudy model. $[Ca]_i$ is varied at 0.1 and 1 mM and $[Na]_i$ at 5, 10, 15, and 20 mM. (*C*) The contributions of calcium entry during normal action potentials (as in Fig. 7) through the reversal of the exchanger by using the Luo-Rudy and Hilgemann models, with varied values of the proportionality correction factor, as explained in the text. The *y* axis indicates the relative contribution of calcium entry through the exchanger current.

larger—not smaller—contributions of the exchanger current to the triggering of calcium release, if the model parameters are not significantly modified.

Sensitivity analysis of model parameters

The contribution of calcium entry via the reversal of the exchanger depends on the accumulation of sodium into the restricted subspace during the upstroke of action potential. Conceivably, more sodium accumulation in the subspace would cause more calcium influx via the exchange. The choice of the exact numerical value of some of the crucial parameters may be assumed to have a dramatic effect on the Na^+-Ca^{2+} exchanger current. Such parameters are the volume of the restricted subspace, the amount of exchanger in subspace (versus the rest of the cell membrane), and the time constant of sodium diffusion. The subspace volume (which we used initially) was estimated as 0.006% of the total cell volume by Jafri et al. (1998), but proposed to be much larger by others: 0.1% by Langer and Peskoff (1996) and 0.13% by Snyder et al. (2000). The large subspace volume would slow the sodium accumulation compared with our basic assumptions. The amount of Na^+-Ca^{2+} exchanger in the subspace membrane was estimated as 20% of the total at the present study, based on the conservative hypothesis of uniform distribution of the exchanger in sarcolemma and the ratio of cleft area/sarcolemmal area of 20%. Finally, the time constant of sodium diffusion was 2 ms, and if larger or smaller, would change the speed of sodium diffusion out of the subspace, and would affect the sodium concentration in it.

We tested the effects of variation of these three crucial parameters on calcium entry through the exchanger in the simulation of normal action potentials (using Luo-Rudy exchanger formulation, initial $[Na^+]_i = 10$ mM), again as the relative contribution of the calcium entry through the exchanger, in the same manner is in show in Fig. 8). The results of these simulations are shown in Fig. 9. If the subspace volume-to-cell-volume ratio is drastically increased the contribution of the exchanger is reduced, but still substantial (~7%), with the highest value used (Fig. 9 *A*). The reduction of the cleft area has a similar effect, wherein halving the area drops the exchanger contribution to ~7% (Fig. 9 *B*). The time constant of sodium diffusion was 2 ms in the basic simulations (corresponding to a value of $2 \cdot 10^{-7}$ cm^2/s, assuming the diffusion distance, 200 nm in the subspace, as given in Langer and Peskoff, 1996). When it was set to be significantly faster the sodium accumulation was much less, and the contribution of the exchanger current subsequently smaller (Fig. 9 *C*). This was not surprising when considering the *I-V* relation of the Na^+-Ca^{2+} exchanger (Fig. 3, *B* and *C*; Fig. 8 *B*). However, the value we used (2 ms) can be regarded as a lower estimate, because several reports (Leblanc and Hume, 1990; Fujioka et al., 1998) suggest much slower diffusion (time constants of up to several

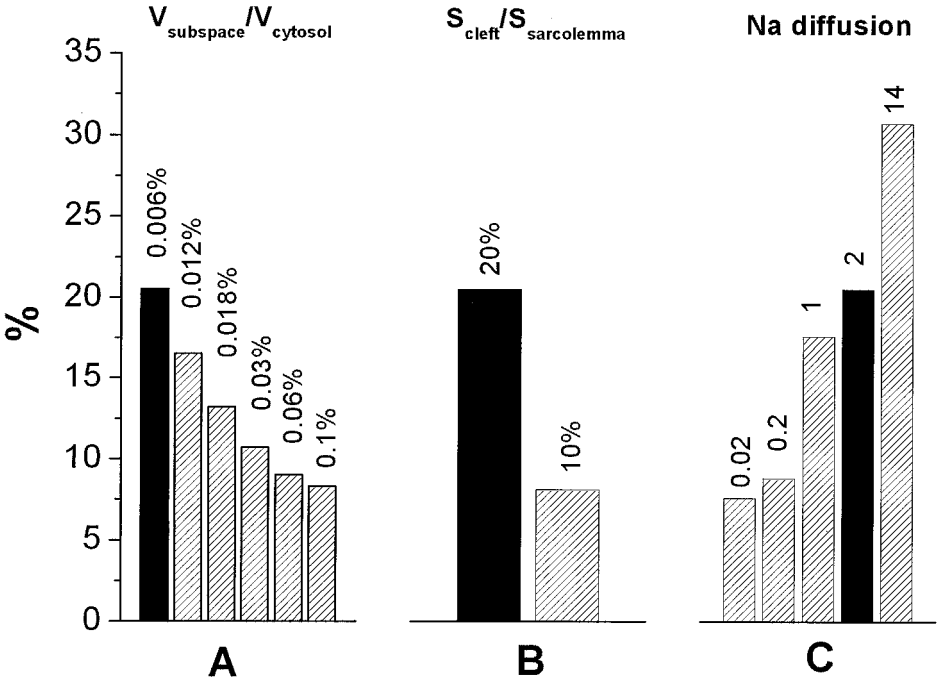

FIGURE 9 Sensitivity analysis of the crucial modeling parameters. The figures show comparison of contributions of calcium entry via the exchanger current during normal action potentials (as in Fig. 7) with varied ratios of (*A*) $V_{subspace}/V_{cytosol}$; (*B*) $A_{cleft}/A_{sarcolemma}$; and (*C*) different sodium diffusion time constants, with the Luo-Rudy model. $V_{subspace}$, volume of the restrict subspace; $V_{cytosol}$, volume of cardiac myocytol; A_{cleft}, surface area of the cleft; $A_{sarcolemma}$, surface area of cardiac sarcolemma. The numbers at the top of each column are the values of the ratios (*A* and *B*) or sodium diffusion time constant (*C*) used in the simulation. The black column in each figure shows the result in the basic simulation analyzed in depth in text.

tens of seconds). The slower Na^+ diffusion would of course enhance the triggering role of the exchanger and, e.g., with a time constant of 14 ms, ~30% of the Ca^{2+} trigger would come via the exchanger current (Fig. 9 *C*).

Thus, even when using quite different estimates for the most crucial parameters in the modeling, the simulations suggest that the exchanger current has a role in the triggering of the Ca^{2+} release. Furthermore, the sensitivity analysis of the parameters treated above shows that they are different in affecting the calcium entry and in triggering calcium release from SR. For example, when the ratio of the subspace volume to cytosolic volume ($V_{subspace}/V_{myocytol}$) increases 17-fold (from 0.1% to 0.006%), the relative contribution of the exchanger current decreases 2.5-fold (from 20.5% to 8.3%), and the sensitivity is 0.14. Similar analysis gives a sensitivity of 1.25 for the ratio of the area of the cleft membrane to the area of the total sarcolemma ($A_{cleft}/A_{sarcolemma}$), and 0.006 for the sodium diffusion time constant. The sensitivity analysis shows that the order of importance of these three parameters in determining the relative contribution of the calcium entry through the exchanger current is 1) the amount of the exchanger molecules in the subspace; 2) the volume of the subspace; and 3) the speed of the sodium diffusion.

DISCUSSION

In this study we have quantitatively evaluated the role of the reverse mode of the Na^+-Ca^{2+} exchanger current in triggering the CICR based on a computer simulation of a mathematical model of the cardiac myocyte. In the model the increase of intracellular calcium concentration causing the CICR takes place in a diffusionally restricted subspace of the cytoplasm, the so-called fuzzy space or dyadic cleft. The main finding of the simulations is that the Na^+-Ca^{2+} exchanger indeed plays a role in triggering the release of calcium from SR. Under conditions where the $[Na^+]_i$ is small, of the order of 10 mM or lower, the reverse mode current is not large enough to trigger the CICR by itself, although it contributes a fraction of the total triggering calcium. However, the contribution of the Na^+-Ca^{2+} exchanger increases up to nearly 100% with the increase of the intracellular sodium concentration and/or positive potential with very clear effects, also on the relative timing of the events. The detailed model of the CICR in the dyadic cleft by Langer and Peskoff (1996; Peskoff and Langer, 1998) predicts larger changes of $[Na^+]_i$ and $[Ca^{2+}]_i$ in the subspace than in our model, reaching maximally above 45 mM for sodium and over 1 mM for calcium near the center of the cleft. In our model the concentration changes are more modest. However, because our model covers the whole of

the myocyte, less details are present, and the spatial dimension in the cleft is omitted. The predictions of our model and the model of Langer and Peskoff do not contradict each other, but our model examines the role of the exchanger in more detail in the whole myocyte.

Validation of the model and simulation methods

The restricted subspace was used in modeling the cardiac E-C coupling by Jafri et al. (1998), and the development of the mathematical model used in the present investigation is based on that model. In our basic model 20% of the Na^+-Ca^{2+} exchanger activity was placed into the subspace membrane. This crucial parameter obviously needs justification. When assuming a uniform distribution of the exchanger molecules in the sarcolemma we arrive at such a figure for the junctional membrane (see Methods). Also, without efficient means for transporting Ca^{2+} from the subspace (leaving the relatively slow diffusion into the bulk cytoplasm as the only means for this) the subspace concentrations would be excessively high. Thus we can take 20% as a starting estimate, meaning that the ratio of L-type calcium conductance to the exchanger currents is the same everywhere in the sarcolemma. The number of exchanger molecules could easily be still higher in the subspace membrane, but while we have no exact numerical data of the exchanger distribution, an approximation has to be made. A smaller amount would mean that the cells are less efficient in regulating calcium and sodium concentrations in the subspace. With this modification this model may be regarded to be more physiological, especially in the description of the CICR. Our model thus gives a useful tool to study the quantitative relationship between the $I_{Ca,L}$ and the $I_{Na\text{-}Ca}$ in causing the CICR, and allows simulation of "ideal experiments," interventions where the pathways of calcium influx through sarcolemma in CICR may be identified and controlled.

The determination of the kind of boundary conditions for the CICR (Fig. 2) in terms of concentration and Ca^{2+} current thresholds was one application of the model. The concept of "clamping" either the concentration or the current also emphasizes the idea inherent in the present modeling, that as far as the CICR in the subspace compartment is concerned, it is irrelevant where the calcium signal originated once the calcium transient has been triggered. The boundary conditions were compared with the *I-V* relationships of the currents (the L-type calcium current and the Na^+-Ca^{2+} exchanger current) in Fig. 3, where also the current threshold for the CICR has been reproduced. In the present simulation of an Na^+/Ca^{2+} *I-V* relation, as shown in Fig. 3, the $I_{Na/Ca}$ under conditions of 20 mM $[Na^+]_i$, 0.1 μM $[Ca^{2+}]_i$, and +40 mV of membrane voltage is 8.5 pA/pF. In experiments in guinea pig ventricular myocytes under similar conditions (Shigematsu and Arita, 1999) the exchanger current was 6.6 pA/pF. In experimental reports the voltage protocols used (Convery and Hancox, 1999) and calcium buffers (Coetzee et al., 1994) may have an effect on the exchanger current. When comparing the exchanger current during the upstroke of action potential we found that the result from our simulation is quite close to the measurement from myocytes. In guinea pig ventricular myocytes, Grantham and Cannell (1996) had $I_{Na/Ca}$ values of 0.55 pA/pF when $I_{Ca,L}$ reached its peak, whereas in our model $I_{Na/Ca}$ is 0.49 pA/pF in the same time. The model *I-V* curves of the currents are thus within the experimental variation, which validates this part of the modeling (see, e.g., McDonald et al., 1986; Watanabe et al., 2001).

Controversies concerning the Na^+/Ca^{2+} exchanger

Although it is clear that L-type Ca^{2+} channels have a dominant role in triggering the CICR, it has been argued that they may not be the only triggers for the Ca^{2+} release from the SR. Since the first reports of Ca^{2+} release from SR that could be triggered by the Na^+-Ca^{2+} exchanger in Ca^{2+} overload conditions (Berlin et al., 1987; Bers et al., 1988), several investigators have shown that Ca^{2+} entry via the reverse mode of the Na^+-Ca^{2+} exchanger could be another triggering mechanism. With high internal Na^+ solution (20 mM), this mechanism has been demonstrated in cat (Nuss and Houser, 1992) and guinea pig ventricular myocytes (Kohmoto et al., 1994), and in lower internal Na^+ concentration in guinea pig (Kohmoto et al., 1994; Vornanen et al., 1994) and rat ventricular myocytes (Levi et al., 1994; Wasserstrom and Vites, 1996). However, several papers report a negligible role for the exchanger, either indirectly (Näbauer et al., 1989) or directly (Sham et al., 1992; Bouchard et al., 1993; Sipido et al., 1997). One problem in interpreting these results is that, as suggested by, e.g., Vornanen et al. (1994), the Na^+-Ca^{2+} exchanger may be much more dependent on temperature than the L-type current, and when experiments are performed at different temperatures, differing results may be obtained. Additionally, the exchanger is dependent on the changes in internal concentrations of sodium and calcium, and those changes are necessarily larger in the restricted subspace than in the rest of the cytosol. Sodium accumulation would favor the exchanger as a trigger, as suggested by Bers et al. (1988), Leblanc and Hume (1990), Carmeliet (1992), and Evans and Cannell (1997). In our simulation, varying the $[Na]_i$ both in voltage-clamp and action potential simulations (Figs. 4–6), the contribution of the exchanger current is greater, the larger the (initial) $[Na]_i$. The triggering efficiency of the exchanger (Fig. 7 *D*) was $<$20% when $[Na]_i$ was below 10 mM, but rose steeply in the function of the $[Na]_i$, reaching values near 100% at 30 mM. A rise in the internal Na^+ concentration also crucially changes the delay (from beginning of voltage change to beginning of the calcium transient), as shown in Fig. 5 *F*. In Sipido et al. (1997) a delay of $\sim$60 ms was found in the

guinea pig in the cytosolic calcium transients with 20 mM $[Na^+]_i$. Our data in Fig. 5 *F* depict the delays for the subspace calcium and, in fact, delays in our model are of the same order as those in Sipido et al. (1997) when the cytosolic transients are observed (Fig. 5 *C*).

One main result of the present study is the confirmation that in the normal, low $[Na]_i$ it is very unlikely that the reverse-mode current of the Na^+-Ca^{2+} exchanger ($I_{Ca,Na-Ca}$) could trigger the CICR if it is the sole external source of calcium. This is in agreement with those investigations with negative findings on the exchanger's role. Equally importantly, we have demonstrated that the reverse mode of the exchanger current contributes to the increase of calcium in the subspace under all conditions studied in the present investigation (Fig. 7 *D*). This would not be the case if the exchanger current were slower than the L-type calcium current. In fact, Ca^{2+} influx through the exchanger into the subspace is always beginning faster than the L-type current in the action potential simulations (Figs. 6 and 7) because of the rapid rise in the $[Na]_i$ in subspace associated with the upstroke of the action potential and the fast sodium (inward) current.

Change of dominant triggering of CICR in elevated $[Na^+]_i$

If we presume that sodium ion distribution in the cytoplasm is uniform, the global sodium concentration increases little following an action potential. During one action potential, the cytoplasmic sodium concentration increased by 0.0137 mM in our model. This is consistent with the estimation by Lederer et al. (1990) that in guinea pig myocytes a 50-nA Na^+ current with an inactivation time constant of 1 ms generates a 0.025 mM increase in sodium concentration. However, with sodium entry into the restricted subspace, a sizable change in $[Na]_i$ occurs (Fig. 6 *C*), as also shown by Langer and Peskoff (1996) in their detailed model of the diffusion and concentration gradients in the subspace. In our model, when the resting $[Na]_i$ is 10 mM, the peak of sodium concentration in the subspace reaches ~30 mM (Fig. 6 *C*), which induces a transient Ca^{2+} entry through the reverse exchange. Under normal action potentials (Figs. 6 and 7) the L-type Ca^{2+} current and the Na^+-Ca^{2+} exchanger current are functioning in synergy. This means that even when the reverse mode of exchanger current is not triggering the CICR it defines the offset, on which the L-type current does the triggering. By this mechanism, the gain of the calcium release would be controlled via the changes in $[Na]_i$ in the subspace, as suggested by Cordeiro et al. (2000). In addition, the calcium currents into the subspace do not simply sum linearly in bringing out the CICR, because the relationship between the open probability of ryanodine receptors and pCa is sigmoidal (Copello et al., 1997; Litwin et al., 1998).

When we observe the relative timing of the integrals of the inward calcium currents via the L-type channels (Fig. 7 *B*) and the exchanger (Fig. 7 *C*), we can conclude that the loading of calcium into the subspace by the exchanger current precedes that of the L-type current, in line with suggestions by Cordeiro et al. (2000). In addition, when the initial $[Na]_i$ is increased, the difference in timing becomes ever larger. When the relative contribution of the exchanger current increases, it causes the threshold for the CICR to be reached earlier. Even when the L-type current contributes more than half of the calcium causing the CICR, the exchanger current is reducing the delay between the action potential upstroke (time 0 ms in Fig. 7) and the calcium transient. One important contribution of the calcium current via the exchanger is, therefore, the timing of the calcium transient with reference to the action potential.

Possible physiological implications

The role of the Na^+-Ca^{2+} exchanger as a trigger for calcium release has numerous implications in physiology of the cardiac myocytes. Considering that $[Na]_i$ is able to regulate the relative contributions of the two different triggers of CICR, any physiological stimulus or medication that changes the $[Na]_i$ will affect the regulation of the calcium release. Hormonal stimuli, such as ET-1-receptor activation (Alvarez et al., 1999), and increase of action potential frequency (Simor et al., 1997) will increase $[Na]_i$, and thus emphasize calcium release triggering via the Na^+/Ca^{2+} exchanger as opposed to via the L-type calcium current. The fact that the delay of the exchange-induced calcium release is radically influenced by $[Na]_i$ in the subspace (Fig. 7 *A*) opens interesting perspectives. An increase of the frequency could influence the electromechanical interval, with a greater contribution of the exchanger-induced calcium release with a reduced delay, being part of adaptational mechanisms making efficient contractions possible in high frequency.

Support from Finnish Heart Research Foundation, Wihuri Foundation, and the Academy of Finland is gratefully acknowledged.

REFERENCES

Alvarez, B. V., N. G. Pérez, I. L. Ennis, M. C. Camilión de Hurtado, and H. E. Cingolani. 1999. Mechanisms underlying the increase in force and Ca^{2+} transient that follow stretch of cardiac muscle: a possible explanation of the anrep effect. *Circ. Res.* 85:716–722.

Berlin, J. R., M. B. Cannell, and W. J. Lederer. 1987. Regulation of twitch tension in sheep cardiac Purkinje fibers during calcium overload. *Am. J. Physiol. Heart Circ. Physiol.* 253:H1540–H1547.

Bers, D. M. 1993. Excitation-Contraction Coupling and Cardiac Contractile Force. Kluwer Academic Publishers, Dordrecht, The Netherlands.

Bers, D. M., D. M. Christensen, and T. X. Nguyen. 1988. Can Ca entry via Na-Ca exchange directly activate cardiac muscle contraction? *J. Mol. Cell. Cardiol.* 20:405–414.

Beuckelmann, D. J., and W. G. Weir. 1988. Mechanisms of release of calcium from sarcoplasmic reticulum of guinea-pig cardiac cells. *J. Physiol.* 405:233–255.

Bouchard, R. A., R. B. Clark, and W. R. Giles. 1993. Role of sodium-calcium exchange in activation of contraction in rat ventricle. *J. Physiol.* 472:391–413.

Cannell, M. B., H. Cheng, and W. J. Lederer. 1995. The control of calcium release in heart muscle. *Science.* 268:1045–1049.

Carmeliet, E. 1992. A fuzzy subsarcolemmal space for intracellular Na^+ in cardiac cells. *Cardiovasc. Res.* 26:433–442.

Coetzee, W. A., H. Ichikawa, and D. J. Hearse. 1994. Oxidant stress inhibits Na-Ca-exchange current in cardiac myocytes: mediation by sulfhydryl groups? *Am. J. Physiol. Heart Circ. Physiol.* 266:H909–H919.

Convery, M. K., and J. C. Hancox. 1999. Comparison of Na^+-Ca^{2+} exchange current elicited from isolated rabbit ventricular myocytes by voltage ramp and step protocols. *Pflügers Arch-Eur. J. Physiol.* 437:944–954.

Copello, J. A., S. Barg, H. Onoue, and S. Fleischer. 1997. Heterogeneity of Ca^{2+} gating in skeletal muscle and cardiac ryanodine receptors. *Biophys. J.* 73:141–156.

Cordeiro, J. M., S. Litwin, and J. H. B. Bridge. 2000. Can NCX rapidly set the gain of EC-coupling without directly triggering SR calcium release in heart. *Biophys. J.* 78:2202.

Eisner, D. A., A. W. Trafford, M. E. Diaz, C. L. Overend, and S. C. O'Neill. 1998. The control of Ca release from the cardiac sarcoplasmic reticulum: regulation versus autoregulation. *Cardiovasc. Res* 38: 589–604.

Evans, A. M., and M. B. Cannell. 1997. The role of L-type Ca^{2+} current and Na^+ current-stimulated Na/Ca exchange in triggering SR calcium release in guinea-pig cardiac ventricular myocytes. *Cardiovasc. Res.* 35:294–302.

Fabiato, A. 1985. Time and calcium dependence of activation and inactivation of calcium-induced release of calcium from the sarcoplasmic reticulum of a skinned canine cardiac Purkinje cell. *J. Gen. Physiol.* 85:247–289.

Fabiato, A., and F. Fabiato. 1975. Concentrations induced by a calcium-triggered release of calcium from the sarcoplasmic reticulum of single skinned cardiac cells. *J. Physiol.* 249:469–495.

Frank, J. S., G. M. D. Reid, R. S. Molday, and K. D. Philipson. 1992. Distribution of the Na^+-Ca^{2+} exchange protein in mammalian cardiac myocytes: an immunofluorescence and immunocolloidal gold-labeling study. *J. Cell Biol.* 2:337–345.

Fujioka, Y., S. Matsuoka, T. Ban, and A. Noma. 1998. Interaction of the Na^+-K^+ pump and Na^+-Ca^{2+} exchange via $[Na^+]_i$ in a restricted space of guinea-pig ventricular cells. *J. Physiol.* 509:457–470.

Ganong, W. F. 1977. Review of Medical Physiology. Lange, Los Altos, California.

Grantham, C. J., and M. B. Cannell. 1996. Ca^{2+} influx during the cardiac action potential in guinea pig ventricular myocytes. *Circ. Res.* 79:194–200.

Jafri, M. S., J. J. Rice, and R. L. Winslow. 1998. Cardiac Ca^{2+} dynamics: the roles of ryanodine receptor adaptation and sarcoplasmic reticulum load. *Biophys. J.* 74:1149–1168.

Kabakov, A. Y. 1998. Activation of K_{ATP} channels by Na/K pump in isolated cardiac myocytes and giant membrane patches. *Biophys. J.* 75:2858–2867.

Kieval, R. S., R. J. Bloch, G. E. Lindenmayer, A. Ambesi, and W. J. Lederer. 1992. Immunofluorescence localization of the Na-Ca exchanger in heart cells. *Am. J. Physiol. Cell Physiol.* 263:C545–C550.

Kohmoto, O., A. J. Levi, and H. B. Bridge. 1994. Relation between reverse sodium-calcium exchange and sarcoplasmic reticulum calcium release in guinea pig ventricular cells. *Circ. Res.* 74:550–554.

Langer, G. A., and A. Peskoff. 1996. Calcium concentration and movement in the diadic cleft space of the cardiac ventricular cell. *Biophys. J.* 70:1169–1182.

Leblanc, N., and J. R. Hume. 1990. Sodium current-induced release of calcium from cardiac sarcoplasmic reticulum. *Science.* 248:372–376.

Lederer, W. J., E. Niggli, and R. W. Hadley. 1990. Sodium-calcium exchange in excitable cells: fuzzy space. *Science.* 248:283.

Levi, A. J., K. W. Spitzer, O. Kohmoto, and J. H. B. Bridge. 1994. Depolarization-induced Ca entry via Na-Ca exchange triggers SR release in guinea pig cardiac myocytes. *Am. J. Physiol. Heart Circ. Physiol.* 266:H1422–H1433.

Lipp, P., and E. Niggli. 1994. Sodium current-induced calcium signals in isolated guinea-pig ventricular myocytes. *J. Physiol.* 474:439–446.

Litwin, S. E., J. Li, and J. H. B. Bridge. 1998. Na-Ca exchanger and the trigger for sarcoplasmic reticulum Ca release: studies in adult rabbit ventricular myocytes. *Biophys. J.* 75:359–371.

Lopez-Lopez, J. R., P. S. Shacklock, C. W. Balke, and W. G. Wier. 1995. Local calcium transients triggered by single L-type calcium channel currents in cardiac cell. *Science.* 268:1024–1045.

Luo, C. H., and Y. Rudy. 1994. A dynamic model of the cardiac ventricular action potential I. Simulation of ionic currents and concentration changes. *Circ. Res.* 74:1071–1096.

Matsuoka, S., and D. W. Hilgemann. 1992. Steady-state and dynamic properties of cardiac sodium-calcium exchange. Ion and voltage dependencies of the transport cycle. *J. Gen. Physiol.* 100:963–1001.

McDonald, T. F., F. A. Cavalie, W. Trautwein, and D. Pelzer. 1986. Voltage-dependent properties of macroscopic and elementary calcium channel currents in guinea pig ventricular myocytes. *Pflugers Arch-Eur. J. Physiol.* 406:437–448.

Näbauer, M., G. Callewaert, L. Cleemann, and M. Morad. 1989. Regulation of calcium release is gated by calcium current, not gating charges, in cardiac myocytes. *Science.* 244:800–803.

Nuss, H. B., and S. R. Houser. 1992. Sodium-calcium exchange-mediated contractions in feline ventricular myocytes. *Am. J. Physiol. Heart Circ. Physiol.* 263:H1161–H1169.

Page, E. 1978. Quantitative ultrastructural analysis in cardiac membrane physiology. *Am. J. Physiol. Cell Physiol.* 235:C147–C158.

Peskoff, A., and G. A. Langer. 1998. Calcium concentration and movement in the ventricular cardiac cell during an excitation-contraction cycle. *Biophys. J.* 74:153–174.

Scriven, R. L., P. Dan, and D. W. Moore. 2000. Distribution of proteins implicated in excitation-contraction coupling in rat ventricular myocytes. *Biophys. J.* 79:2682–2691.

Sham, J. S., L. Cleemann, and M. Morad. 1992. Gating of the cardiac Ca^{2+} release channel: the role of Na^+ current and Na^+-Ca^{2+} exchange. *Science.* 255:850–853.

Shigematsu, S., and M. Arita. 1999. Anoxia depresses sodium-calcium exchange currents in guinea-pig ventricular myocytes. *J. Mol. Cell. Cardiol.* 31:895–905.

Simor, T. S., T. Lorand, B. Gaszner, and G. A. Elgavish. 1997. The modulation of pacing-induced changes in intracellular sodium levels by extracellular Ca^{2+} in isolated perfused rat hearts. *J. Mol. Cell. Cardiol.* 29:1225–1235.

Sipido, K. R., M. Maes, and F. V. Werf. 1997. Low efficiency of Ca^{2+} entry through the Na^+-Ca^{2+} exchanger as trigger for Ca^{2+} release from the sarcoplasmic reticulum. *Circ. Res.* 81:1034–1044.

Snyder, S. M., B. M. Palmer, and R. L. Moore. 2000. A mathematical model of cardiocyte Ca^{2+} dynamics with a novel representation of sarcoplasmic reticular Ca^{2+} control. *Biophys. J.* 79:94–115.

Stern, M. D. 1992. Theory of excitation-contraction coupling in cardiac muscle. *Biophys. J.* 63:497–517.

Sun, X. H., F. Protasi, M. Takahashi, H. Takeshima, D. G. Ferguson, and C. Franzini-Armstrong. 1995. Molecular architecture of membranes involved in excitation-contraction coupling of cardiac muscle. *J. Cell. Biol.* 291:659–671.

Varghese, A., and G. S. Sell. 1997. A conservation principle and its effect on the formulation of Na-Ca exchanger current in cardiac cells. *J. Theor. Biol.* 189:33–40.

Vornanen, M., N. Shepherd, and G. Isenberg. 1994. Tension-voltage relations of single myocytes reflect Ca release triggered by Na/Ca exchange at 30°C but not 23°C. *Am. J. Physiol. Cell Physiol.* 267:C623–C633.

Wasserstrom, J. A., and A. M. Vites. 1996. The role of Na^+-Ca^{2+} exchange in activation of excitation-contraction coupling in rat ventricular myocytes. *J. Physiol.* 493:529–542.

Watanabe, Y., T. Iwamoto, I. Matsuoka, S. Ohkubo, T. Ono, T. Watano, M. Shikegawa, and J. Kimura. 2001. Inhibitory effect of 2,3-butanedione monoxime (BDM) on Na^+/Ca^{2+} exchange current in guinea-pig cardiac ventricular myocytes. *Br. J. Pharmacol.* 132:1317–1325.

Wendt-Gallitelli, M. F., T. Voigt, and G. Isenberg. 1993. Microheterogeneity of subsarcolemmal sodium gradient: electron probe microanalysis in guinea-pig ventricular myocytes. *J. Physiol.* 472:33–44.